BJ www.biochemj.org

BJ Structure

Biochem. J. (2011) **434**, 143–151 (Printed in Great Britain) doi:10.1042/BJ20101895

Flexibility of the Ure2 prion domain is important for amyloid fibril formation

Yong YU*†[1,2], Hai-Yan WANG*†[1], Ming BAI*[3] and Sarah PERRETT*[4]

*National Laboratory of Biomacromolecules, Institute of Biophysics, Chinese Academy of Sciences, 15 Datun Road, Chaoyang District, Beijing 100101, China, and †Graduate University of the Chinese Academy of Sciences, 19 Yuquan Road, Shijingshan District, Beijing 100049, China

Ure2, the protein determinant of the *Saccharomyces cerevisiae* prion [*URE3*], has a natively disordered N-terminal domain that is important for prion formation *in vivo* and amyloid formation *in vitro*; the globular C-domain has a glutathione transferase-like fold. In the present study, we swapped the position of the N- and C-terminal regions, with or without an intervening peptide linker, to create the Ure2 variants CLN-Ure2 and CN-Ure2 respectively. The native structural content and stability of the variants were the same as wild-type Ure2, as indicated by enzymatic activity, far-UV CD analysis and equilibrium denaturation. CLN-Ure2 was able to form amyloid-like fibrils, but with a significantly longer lag time than wild-type Ure2; and the two proteins were unable to cross-seed. Under the same conditions, CN-Ure2 showed limited ability to form fibrils, but this was improved after addition of 0.03 M guanidinium chloride. As for wild-type Ure2, allosteric enzyme activity was observed in fibrils of CLN-Ure2 and CN-Ure2, consistent with retention of the native-like dimeric structure of the C-domains within the fibrils. Proteolytically digested fibrils of CLN-Ure2 and CN-Ure2 showed the same residual fibril core morphology as wild-type Ure2. The results suggest that the position of the prion domain affects the ability of Ure2 to form fibrils primarily due to effects on its flexibility.

Key words: amyloid, mutant, protein folding, sequence permutation, Ure2p, yeast.

INTRODUCTION

Ure2 is the protein determinant of the non-chromosomal genetic element [*URE3*] in *Saccharomyces cerevisiae* [1]. Analogous to the properties of the mammalian prion protein, a conformational change in the Ure2 protein to an aggregated form gives rise to the [*URE3*] prion state [2] and Ure2 readily forms amyloid-like fibrils *in vitro* [3,4]. The N-terminal region of Ure2 (residues 1–89) is termed the PrD (prion domain) as it is necessary for prion or amyloid formation [2,3,5]. The PrD of Ure2 is largely unstructured in the native state [4,6,7]. The C-terminal region of Ure2 (residues 90–354) has a globular fold with similarity to GSTs (glutathione transferases) [8,9].

Despite its similarity to GSTs, the Ure2 protein lacks activity towards GST substrates, although a single amino acid change in the active site is sufficient to introduce GST activity into the Ure2 protein [10]. The normal soluble form of Ure2 is dimeric [3,4,6] and has a regulatory function in the nitrogen catabolite repression pathway involving interaction with the transcription factor Gln3 [11]; this regulatory function is lost on conversion into the prion state [1]. The presence of the URE2 gene also conveys protection to yeast cells against heavy metal and oxidant toxicity, and interestingly this protective function is maintained in the prion state [12]. Consistent with this, Ure2 has both GPx (glutathione-dependent peroxidase) and GRX (glutaredoxin) activities *in vitro*, and the enzymatic activity is maintained on conversion of the protein into the fibrillar form [13,14]. Although the C-terminal domain is necessary and sufficient for the regulatory function of Ure2 [15], the presence of the N-terminal PrD enhances this function *in vivo* [16]. Likewise, the presence of the N-terminal region affects the enzymatic activity of native Ure2 *in vitro*, although in this case, shortening or removal of the N-terminal domain enhances activity [10,14]. Deletions or mutations in the C-terminal domain have been found to affect induction of the prion state when the mutant is expressed in a WT (wild-type) background [2,17,18] and can alter the biophysical properties of the fibrils formed [19]. However, the presence of the N-terminal domain has no effect on the thermodynamic stability or folding pathway of the C-terminal domain [6,19–21], and no direct interaction between the N- and C-terminal domains has so far been detected [7]. This suggests that from a structural point of view, the N- and C-terminal regions of Ure2 are essentially independent.

The interesting finding that the enzymatic activity of Ure2 is maintained within the fibrils [10,13,14] is consistent with a previous report indicating that the α-helical content of the fibrils is similar to that in the native dimer and the ability to bind GSH is maintained in the fibrils [22]. However, in other respects, fibrils of Ure2 exhibit many of the characteristics of amyloid in that they are resistant to proteolysis, show yellow–green birefringence in polarized light when bound to Congo Red [3], and show a cross-β pattern by X-ray diffraction [23]. It had been suggested in a preliminary model that fibril assembly involves dissociation of the dimeric C-terminal domain and repacking of the monomers in a manner that involves non-native interactions between the N- and C-terminal domains [22]. However, this suggestion is somewhat at odds with the extreme stability of the Ure2 dimer [20] and subsequent studies of cysteine mutants indicate that the relative arrangement of the C-terminal domains within fibrils is similar to that in the native dimer [24]. Furthermore, when monitoring the kinetics of GRX activity, the same allostery is observed in fibrils as in the native dimer, and the minimum catalytic unit for Ure2

Abbreviations used: CHP, cumene hydroperoxide; GdmCl, guanidinium chloride; GPx, glutathione-dependent peroxidase; GRX, glutaredoxin; GST, glutathione transferase; HEDS, 2-hydroxyethyl disulfide; PrD, prion domain; ThT, thioflavin T; WT, wild-type.

[1] These authors contributed equally to this work.

[2] Present address: Department of Cell Biology, Harvard Medical School, 240 Longwood Avenue, Boston, MA 02115, U.S.A.

[3] Present address: Department of Medicine, Harvard Medical School, and Division of Rheumatology, Immunology and Allergy, Brigham and Women's Hospital, Boston, MA 02115, U.S.A.

[4] To whom correspondence should be addressed (email sarah.perrett@cantab.net).

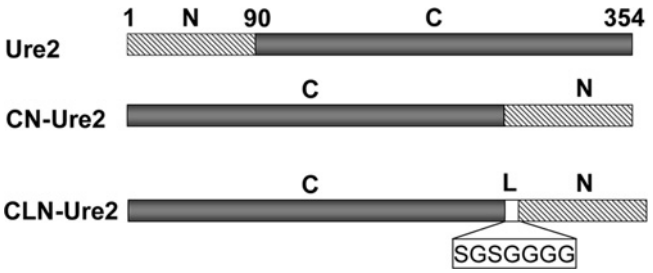

Figure 1 Domain structure of WT-Ure2, CN-Ure2 and CLN-Ure2

Schematic diagram showing the positions of the N-terminal PrD (N), the C-terminal GST-like domain (C) and insertion of a flexible linker (L).

is a dimer in both its soluble and fibrillar forms, indicating that the C-terminal domains of Ure2 are arranged as functional dimers within the fibrillar arrays [14].

Comparison of a range of chimaeras between the Ure2 PrD and various globular enzymes shows that the PrD is capable of forming fibrils with a range of different appended C-terminal domains in place of the Ure2 GST-like domain [25]. Consistent with the findings for Ure2 itself [10,13,14], the enzymatic activity of the C-terminal domains in the chimaeric fibrils is maintained [25], suggesting a common architecture. When fibrils of Ure2 or its chimaeras are digested with proteinase K, in each case a similar residual core of approx. 5 nm in diameter is observed, suggesting that Ure2 and its chimaeras consist of a central amyloid core surrounded by the globular functional C-terminal domains [26]. Taken together, the data are consistent with a model where the Ure2 PrD forms a central core with amyloid properties, whereas the GST-like domains of Ure2 are maintained in a native dimeric conformation outside this core.

In order to study the effect of the position of the PrD on amyloid fibril formation, we constructed two Ure2 variants, which we termed CN-Ure2 and CLN-Ure2 (see Figure 1). Using these variants, we demonstrated that changing the position of the PrD did not influence the structure or function of the C-terminal domain of Ure2. However, the position of the Ure2 PrD strongly influenced the ability to form amyloid-like fibrils, and the results suggest that the flexibility of the PrD plays an important role in this. The results of cross-seeding experiments suggest that swapping the relative positions of the domains forces a change in the overall architecture of CLN-Ure2 fibrils compared with WT. On the other hand, digestion of the variant fibrils indicated a similar core structure as for WT fibrils and, using the GRX activity assay, we observed allostery between the dimer subunits in fibrils of CN-Ure2 and CLN-Ure2 indicating that, in terms of these key aspects, the molecular arrangement of the monomers within the fibrils is similar to that in WT-Ure2.

EXPERIMENTAL

Materials

Tris/HCl, sodium azide, GSH, NADPH, CHP (cumene hydroperoxide), GdmCl (guanidinium chloride) and ThT (thioflavin T) were from Sigma. All other reagents were local products of analytical grade. Molecular-biology enzymes were from TaKaRa. Solutions were prepared volumetrically; the concentration of GdmCl solutions was confirmed using an Abbe refractometer. Double-deionized water was used throughout.

Cloning, expression and protein purification

Primers used in the contruction of CN-Ure2 were Primer A, 5′-GTGGTGAAATGAACAACAACGGTAACCA-3′; Primer B, 5′-GGCCGCAAGCTTCTAAGCCTGCTGCTGCTGA-3′; Primer C, 5′-GGCCGCGGATCCATGTTCTCTGACATGTCTCACGT-3′; Primer D, 5′-TTGTTCATTTCACCACGCAGAGCTTT-3′; Primer E, 5′-GCTCTGCGTGGTGAAAGCGGTAGCGGTGGT-GGTGGTATGAACAACAACGGT-3′; and Primer F, 5′-ACCG-TTGTTGTTCATACCACCACCACCGCTACCGCTTTCACCA-CGCAGAGC-3′. The cDNA of CN-Ure2 was constructed by PCR using a synthetic WT-Ure2 gene as the template [6] as follows. The N-terminal region was amplified using Primers A and B, and the C-terminal region was amplified using Primers C and D. Then, using the two fragments as templates, Primers A and D were used to obtain CN-Ure2. CLN-Ure2 was constructed using CN-Ure2 as the template, using Primers E and F to introduce the SGSGGGG peptide linker between the two protein domains. The integrity of the mutants was verified by DNA sequencing.

All of the proteins were expressed in *Escherichia coli* with a short N-terminal His_6 tag to allow a high level of purity to be achieved. WT-Ure2, CN-Ure2 and CLN-Ure2 were purified under native conditions by nickel-affinity chromatography as described previously [6], except that in each case a French press was used to lyse cells in place of sonication. Proteins were stored at $-80\,^{\circ}C$ and defrosted in a 25 °C water bath immediately prior to use. Samples were prepared in 50 mM Tris/HCl (pH 8.4) containing 0.2 M NaCl and centrifuged at 22000 ***g*** for 30 min at 4 °C to remove any aggregates.

Analytical size-exclusion chromatography

Under the conditions used in the present study, Ure2 is dimeric in its native state [6]. The dimeric structure of CN-Ure2 and CLN-Ure2 was confirmed by size-exclusion chromatography using an Äkta fast protein liquid chromatography system (Amersham Biosciences) with a Superdex 200 10/300 GL column equilibrated in 50 mM Tris/HCl (pH 8.4) containing 0.2 M NaCl at room temperature (approx. 25 °C), using a flow rate of 0.5 ml/min. In each case, 1 ml of 20 μM protein was loaded.

Far-UV CD measurements

CD spectra were recorded over the range 200–260 nm in a Pistar-180 Spectrometer (Applied Photophysics). Proteins were first centrifuged at 22000 ***g*** for 30 min to remove large aggregates. Spectra of 50 μM WT-Ure2, CN-Ure2 and CLN-Ure2 were measured at 25 °C in a 0.1 mm path-length thermostatically maintained cuvette. Data were acquired at a step size of 0.5 nm. For each sample, the mean residue ellipticity was reported as an average of three scans.

Equilibrium denaturation

All equilibrium folding experiments were performed in 50 mM Tris/HCl (pH 8.4) containing 0.2 M NaCl. GdmCl was used as the denaturant as described previously [6,21]. Samples containing different concentrations of GdmCl were prepared and allowed to equilibrate overnight at 25 °C before taking measurements. All measurements were performed at 25 °C in a thermostatically maintained cuvette using a Shimadzu RF-5301PC spectrofluorimeter. Excitation was at 280 nm and emission spectra were measured between 300 nm and 400 nm. Excitation and emission slit widths were set at 5 nm. The maximum

change in intensity on denaturation is observed at 327 nm and under apparent two-state conditions, an isosbestic point at 369 nm is observed [6,21]. The final concentration of protein in the denaturation samples was 1 μM.

Assay of enzymatic activity

The GPx activity of WT-Ure2, CN-Ure2 and CLN-Ure2 was determined using GSH with CHP as the hydroperoxide substrate, using a coupled spectrophotometric assay as described previously [13,27]. Unless otherwise indicated, the assay was carried out at 25 °C in a 1 ml reaction volume containing 100 mM sodium phosphate (pH 7.5), 4 mM sodium azide, 1.0 mM GSH, 0.15 mM NADPH, 0.24 units of glutathione reductase and 0.3−3.0 μM protein. The reaction mixture was pre-incubated at 25 °C for 6 min, after which the reaction was started by the addition of CHP to a final concentration of 1.2 mM. The progress of reactions was monitored continuously by following the decrease in NADPH absorbance at 340 nm on a Shimadzu UV2501 spectrophotometer. Initial velocities were determined from the linear slope of progress curves obtained with a molar absorption coefficient for NADPH of 6220 $M^{-1} \cdot cm^{-1}$ after subtracting the non-enzymatic velocities due to the auto-oxidation of GSH by the hydroperoxide determined from the corresponding blank.

Using GSH and HEDS (2-hydroxyethyl disulfide) as substrates, the GRX activity of WT-Ure2, CN-Ure2 and CLN-Ure2 was determined in a spectrometric coupled assay at 25 °C, as described previously [14,28]. Typically, a 1 ml reaction volume in a cuvette containing 100 mM sodium phosphate buffer (pH 7.5), 0.2−5.0 mM GSH, 0.2−5.0 mM HEDS, 0.25−0.8 units/ml glutathione reductase, 0.2 mM NADPH and 1 mM EDTA was pre-incubated at 25 °C for 2 min. The enzyme (WT-Ure2, CN-Ure2 or CLN-Ure2) was then added to the cuvette to trigger the reaction. The final enzyme concentration was 0.1−1.0 μM for soluble proteins and the maximal concentration of fibrils was 2.0 μM. The activity was measured from the continuous decrease of NADPH absorption at 340 nm for 5 min. All initial velocities were corrected by subtraction of the non-enzymatic reaction measured using an equivalent volume of buffer in place of the protein solution. The data were fit to the Michaelis−Menten equation or the Hill equation, as described previously [14,28].

Amyloid formation

The kinetics of amyloid formation of Ure2 and its variants was monitored using ThT-binding fluorescence and incubation was at a constant temperature of 37 °C with shaking, as described previously [21,29,30]. Proteins were prepared in 50 mM Tris/HCl buffer (pH 8.4), containing 0.2 M NaCl and the protein concentration was 30−50 μM. At regular time intervals, 10 μl aliquots were removed from the reaction mixture and assayed for ThT binding. After mixing, the fluorescence of ThT dye was measured at 482 nm using an excitation wavelength of 450 nm. Samples for direct comparison were incubated in parallel. Each reaction was performed in triplicate and the results averaged. In the seeded reaction, a small amount [5 % (w/w)] of preformed fibrillar aggregates was sonicated and added to freshly buffered protein solution as described previously [31], and the kinetics of fibril formation were followed as described above. Fibrils for enzyme activity experiments were grown under the same conditions as described above and collected by centrifugation (15 000 ***g*** for 30 min at 4 °C), as described previously [10,13,14].

Digestion of amyloid fibrils

Proteinase K-digested fibrils were prepared essentially as described previously [26]. In brief, fibrils of WT-Ure2, CN-Ure2 or CLN-Ure2 were grown as described above. Once the ThT value had reached a plateau, proteinase K was added to give a final concentration of 0.1 mg/ml, and the samples were incubated at 37 °C for 16 h. The digested fibrils were then collected by centrifugation (15 000 ***g*** for 30 min at 4 °C), washed once with 50 mM Tris/HCl buffer (pH 8.4), containing 0.2 M NaCl, and then resuspended in the same buffer for further analysis by electron microscopy.

Electron microscopy

Fibril samples were loaded on to a 200 mesh copper electron microscopy grid coated with a formvar film. To avoid rapid desiccation, sedimentation was allowed to take place during a 10−30 min period in a moist Petri dish. The grids were then rinsed with 15−20 drops of freshly prepared 1 % uranyl acetate in water (passed through a 0.22 μm filter, Millipore), dried with filter paper, and observed with a Phillips Tecnai 20 electron microscope at 100 kV.

RESULTS

CN-Ure2 and CLN-Ure2 are dimeric and have the same overall secondary structure as WT-Ure2

Ure2 consists of a relatively flexible and protease-sensitive N-terminal region and a globular C-terminal region [32]. In order to investigate how the relative positions of the N- and C-terminal regions might affect the properties of the Ure2 protein, we constructed a permutation mutant, CN-Ure2, in which the relative positions of these two regions were swapped (Figure 1). We also constructed a second mutant, CLN-Ure2, in which a flexible hepta-peptide linker was inserted between the two regions (Figure 1). Size-exclusion chromatography of the two mutants showed that the elution time was indistinguishable from that of WT-Ure2 (Figure 2), indicating that both CN-Ure2 and CLN-Ure2, like WT-Ure2 [3,4,6], are dimeric, with a similar hydrodynamic radius.

To compare the secondary structure of WT-Ure2, CN-Ure2 and CLN-Ure2, we recorded their CD spectra in the far-UV range, under identical conditions. The results showed that the α-helical content of the three proteins was the same (Figure 3), indicating that exchanging the positions of the N-terminal and C-terminal regions does not disrupt the secondary structure of the Ure2 protein.

CN-Ure2 and CLN-Ure2 show the same thermodynamic stability as WT-Ure2

In order to investigate whether swapping the positions of the N- and C-terminal regions might have any effect on the stability or folding of Ure2, we performed equilibrium denaturation of CN-Ure2 and CLN-Ure2 and compared the results to those obtained for WT-Ure2 under identical conditions. As described previously for the WT protein [6,21], under the conditions used in the present study [50 mM Tris/HCl (pH 8.4), containing 200 mM NaCl at 25 °C], Ure2 showed a single unfolding transition. The unfolding curves of the mutants CN-Ure2 and CLN-Ure2 were indistinguishable from that of the WT protein (Figure 4), consistent with the lack of contribution of the prion domain to the stability or folding properties of the protein [6,19−21].

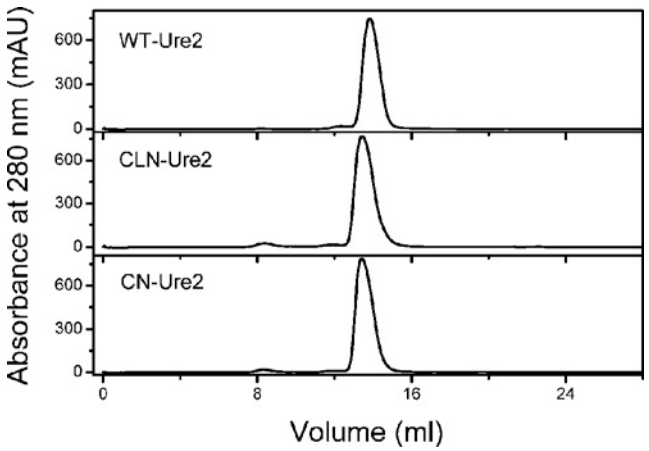

Figure 2 Size-exclusion chromatography analysis of WT-Ure2, CN-Ure2 and CLN-Ure2

Conditions were 50 mM Tris/HCl buffer (pH 8.4), containing 0.2 M NaCl at room temperature using a Superdex 200 10/300 GL column and running at a flow rate of 0.5 ml/min. In each case, 1 ml of 20 μM protein was loaded. mAU, milli absorbance units.

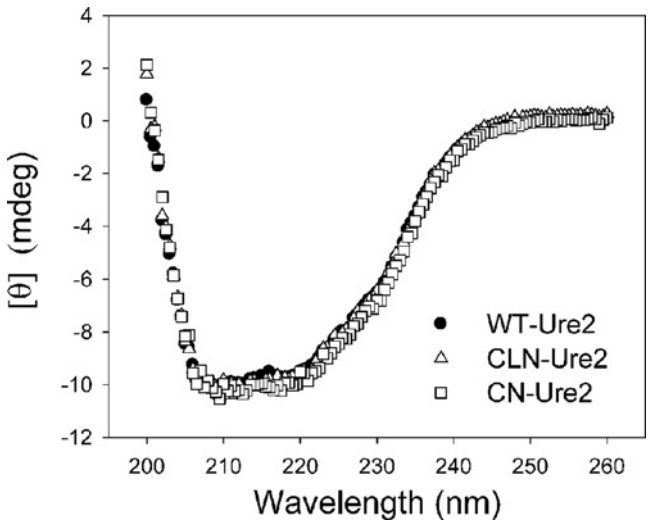

Figure 3 Structural comparison of WT-Ure2, CN-Ure2 and CLN-Ure2 by far-UV CD

The protein concentration was 50 μM in 50 mM Tris/HCl buffer (pH 8.4), containing 0.2 M NaCl at 25 °C.

The enzymatic activity of CN-Ure2 and CLN-Ure2 is similar to that of WT-Ure2 in both soluble and fibrillar forms

The C-terminal region of Ure2 was identified as belonging to the GST family on the basis of sequence similarity [15], structure [8,9] and activity [10,13,14]. The ability of CN-Ure2 and CLN-Ure2 to reduce hydroperoxides (i.e. show GPx activity) was tested *in vitro* using purified CN-Ure2 or CLN-Ure2 with the oxidant substrate CHP, and the reducing agent GSH. Reactions were followed by the oxidation of NADPH, which is coupled to the reduction of GSSG to GSH by glutathione reductase. The rate of non-enzymatic oxidation of NADPH in the absence of CN-Ure2 or CLN-Ure2 was subtracted in each case. As described previously for the WT protein [13], we used pH 7.5 and 25 °C as the standard conditions to measure the GPx activity of CN-Ure2 and CLN-Ure2. When CN-Ure2 or CLN-Ure2 was added in the presence of all of the other components of the assay, a significant

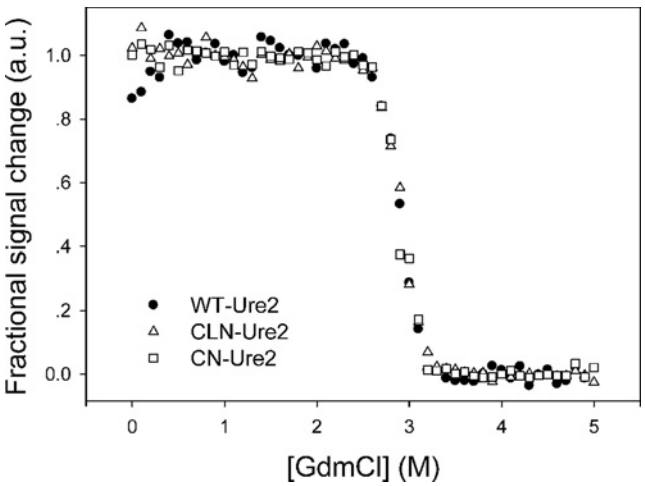

Figure 4 Equilibrium denaturation of WT-Ure2, CN-Ure2 and CLN-Ure2

The conditions were 50 mM Tris/HCl buffer (pH 8.4), containing 0.2 M NaCl, 1 μM of WT-Ure2 (●), CN-Ure2 (□) or CLN-Ure2 (Δ) and different concentrations of GdmCl as indicated, at 25 °C. a.u., arbitrary units.

increase in the oxidation rate of NADPH was observed and the initial velocity of the CN-Ure2- or CLN-Ure2-catalysed reaction was found to be proportional to the protein concentration (Figure 5a). This demonstrates that CN-Ure2 and CLN-Ure2 have GSH-dependent peroxidase activity, and the level of activity is the same within error as that of WT-Ure2 (Figure 5b).

In order to investigate this further, we used the recently discovered GRX activity of Ure2, as the GRX activity assay has greater sensitivity than the GPx activity assay, and allows observation of allostery within the Ure2 dimer in both the soluble and fibrillar forms of the protein [14]. We compared the steady-state kinetic parameters for the GRX activity of CN-Ure2 and CLN-Ure2 with those previously measured for the WT-Ure2 protein (Table 1). The results were consistent with those of the GPx activity, and indicated that transferring the PrD of Ure2 from the N-terminus to the C-terminus affects neither its native activity nor its allosteric behaviour (Figures 6a and 6b).

As the GRX assay is sufficiently sensitive to allow measurement of kinetic parameters in the fibrillar state [14], we also applied this assay to fibrils of CN-Ure2 and CLN-Ure2. The mutants, particularly CN-Ure2, were found to form fibrils less readily than the WT-Ure2 protein (see below). However, after prolonged incubation, a sufficient yield of fibrils was obtained to conduct the GRX activity assay (Figures 6c and 6d). The parameters that were obtained are shown in Table 1. As for the dimeric forms of the proteins, the parameters obtained for fibrils of CN-Ure2 and CLN-Ure2 were similar to those for WT-Ure2 (Table 1).

Fibrils of CN-Ure2 and CLN-Ure2 show a similar core structure to that of WT-Ure2 after digestion with proteinase K

It has been noted previously that after digestion with proteinase K, Ure2 fibrils maintain a fibrillar appearance, but with a reduced diameter compared with undigested fibrils [22,26]. Digestion of a range of chimaeras formed from the Ure2 PrD with other globular proteins appended at the C-terminus form residual fibril cores that are indistinguishable in morphology from that of WT-Ure2 [26]. In the present study, we prepared fibrils of WT-Ure2, CN-Ure2 and CLN-Ure2 (Figure 7a), and subjected them to proteinase K digestion (Figure 7b). The resulting fibril

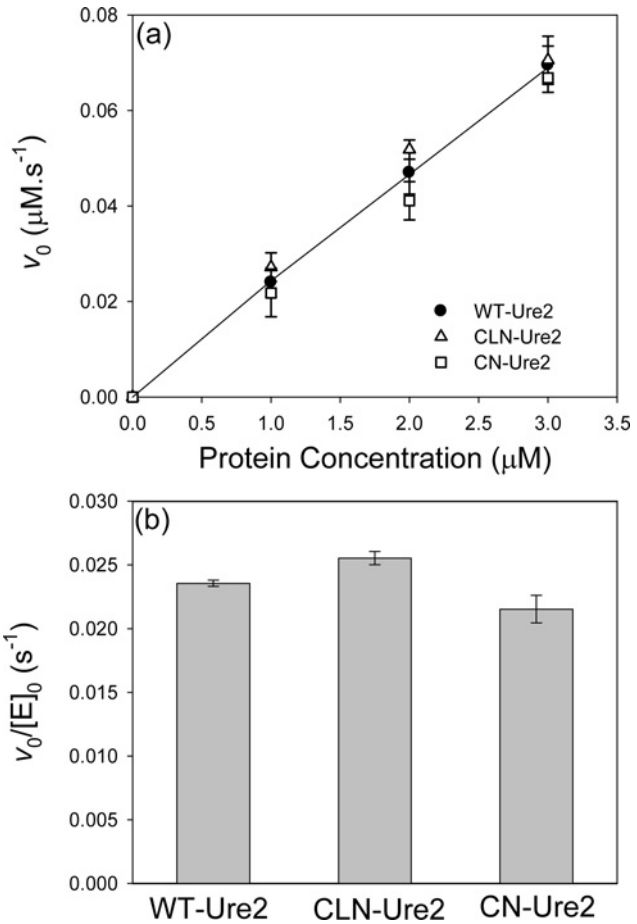

Figure 5 Comparison of the GPx activity of WT-Ure2, CN-Ure2 and CLN-Ure2

The reaction conditions were 100 mM sodium phosphate buffer (pH 7.5), 1 mM GSH and 1.2 mM CHP at 25 °C. (**a**) The initial velocity of the WT-Ure2, CN-Ure2 or CLN-Ure2 catalysed reaction show the same increase with increasing protein concentration. (**b**) WT-Ure2, CN-Ure2 and CLN-Ure2 have similar levels of GPx activity.

cores were morphologically indistinguishable from each other (Figure 7), or from those previously reported for WT-Ure2 [26], suggesting that CLN-Ure2 and CN-Ure2 share the same amyloid core structure as WT-Ure2.

CN-Ure2 and CLN-Ure2 show reduced ability to form amyloid-like fibrils compared with WT-Ure2 due to reduced flexibility of the PrD

ThT binding provides a convenient method to assay the effect of different factors on the kinetics of amyloid formation for Ure2 [21,29]. We compared the ThT-monitored kinetics of amyloid formation for WT-Ure2, CN-Ure2 and CLN-Ure2. As described previously [3,4], WT-Ure2 rapidly forms fibrils *in vitro* and the lag phase of fibril formation can be circumvented by seeding with pre-formed fibrillar seeds of WT-Ure2 (Figure 8a). Under the same conditions, the ThT-binding fluorescence of CLN-Ure2 showed a sigmoidal time course similar to that for WT-Ure2, but with a longer lag time and the ThT value of the plateau was reduced (Figure 8b). In contrast, CN-Ure2 incubated under the same conditions showed very little increase in ThT fluorescence (Figure 8c) and far fewer fibrils could be detected by electron microscopy or atomic force microscopy (results not shown). In order to test whether the structure of the fibrils was the same for WT- and CLN-Ure2, we tested whether pre-formed fibrillar seeds of CLN-Ure2 were able to seed formation of WT-Ure2 fibrils (Figure 8a) and vice versa (Figure 8b). In both cases, self-seeding gave a clear reduction in the lag time, whereas cross-seeding was identical with the control in the absence of seed (Figures 8a and 8b). CLN-Ure2 was found to cross-seed formation of CN-Ure2 fibrils, but the yield was still very low (results not shown). These results indicate that changing the position of the PrD to the C-terminus of Ure2 reduces its ability to form fibrils, but this can be mitigated by insertion of a flexible linker between the two domains. The lack of cross-seeding between WT- and CLN-Ure2 indicates that the difference in the relative arrangement of the N- and C-terminal domains in the two types of fibrils prevents co-polymerization.

In order to investigate further the role of flexibility of the PrD in the ability of Ure2 to form fibrils, we added low concentrations of the chemical denaturant GdmCl to the fibril-formation assay. Ure2 is a relatively stable protein, and under the conditions used in the present study, does not show any significant degree of

Table 1 Apparent steady-state kinetic parameters and Hill coefficients for the GRX activity of soluble dimer and fibrils of WT-Ure2, CN-Ure2 and CLN-Ure2

ND, not determined.

	Fixed [GSH] at 1 mM*		Fixed [HEDS] at 3 mM†		
Protein	$K_{m(HEDS)}$(app) (mM)	V_{max}(app)/$[E]_0$ (s^{-1})	n_H	$[GSH]_{0.5}$ (mM)	V_{max}(app)/$[E]_0$ (s^{-1})
Dimeric protein					
WT-Ure2‡	2.4 ± 0.1	0.32 ± 0.02	2.0 ± 0.1	2.3 ± 0.1	1.0 ± 0.1
CN-Ure2	2.4 ± 0.3	0.38 ± 0.02	2.1 ± 0.1	2.1 ± 0.1	1.1 ± 0.1
CLN-Ure2	2.1 ± 0.4	0.39 ± 0.01	2.1 ± 0.1	2.1 ± 0.1	1.1 ± 0.1
Fibrils					
WT-Ure2‡	2.2 ± 0.2	⩾0.16 ± 0.01§	1.7 ± 0.1	2.3 ± 0.1	⩾0.40 ± 0.02§
CN-Ure2	ND	ND	1.6 ± 0.2	3.0 ± 0.6	⩾0.46 ± 0.07§
CLN-Ure2	ND	ND	1.9 ± 0.3	1.8 ± 0.3	⩾0.21 ± 0.03§

*The errors shown are the S.E.M. for at least three independent measurements.

†The errors shown are the standard error of the fit to the Hill equation.

‡Data taken from Zhang and Perrett [14].

§The values were calculated according to the maximum Ure2 concentration in fibrils, on the assumption that all soluble Ure2 was converted into amyloid-like fibrils. These are therefore minimum values for $V_{max}/[E]_0$, as the actual concentration of Ure2 in fibrils may be lower, due to formation of amorphous aggregates [14].

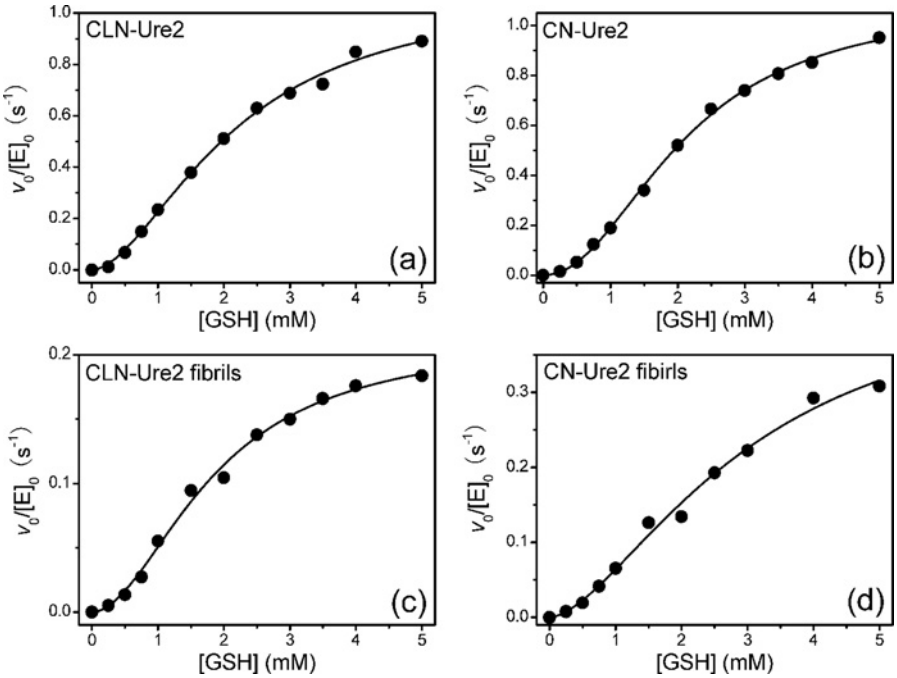

Figure 6 GRX activity for soluble and fibrillar CN-Ure2 and CLN-Ure2

The reaction conditions used were 0.2 mM NADPH and 1 mM EDTA in 100 mM sodium phosphate buffer (pH 7.5) at 25 °C, with various concentrations of GSH and 3.0 mM HEDS. The samples were pre-incubated at 25 °C for 2 min. The protein concentrations were 0.8 μM for soluble CLN-Ure2 (**a**) and CN-Ure2 (**b**), and 1.2 μM for fibrillar CLN-Ure2 (**c**) and CN-Ure2 (**d**). The fit to the Hill equation is shown (solid lines). The parameters obtained from the fits are shown in Table 1.

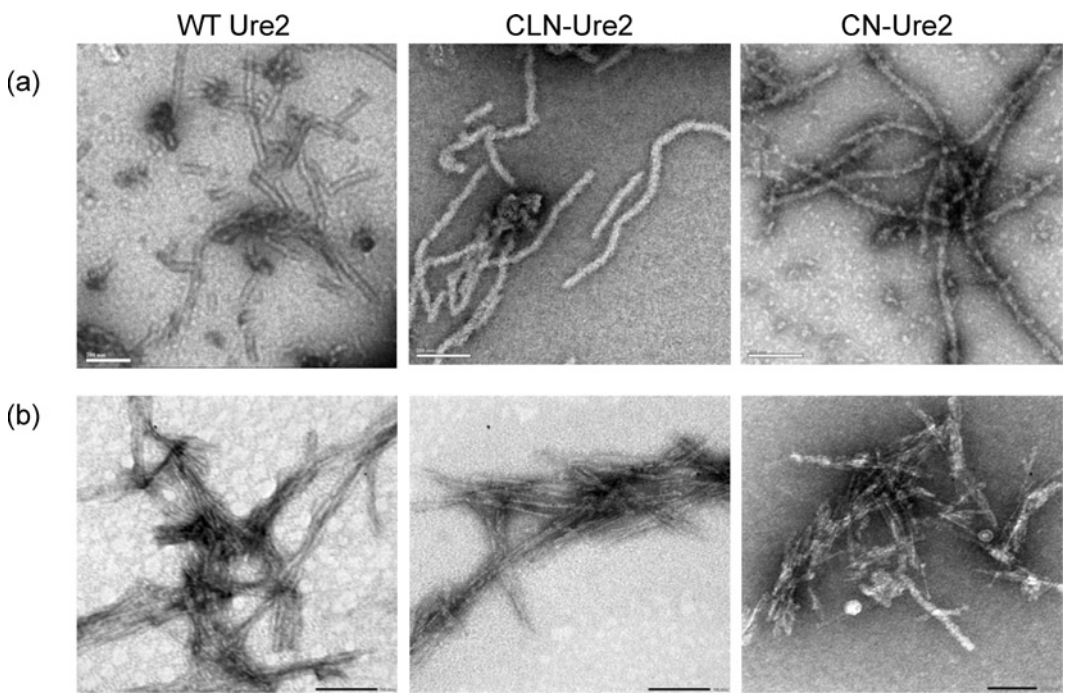

Figure 7 Electron micrographs of fibrils of WT-Ure2, CN-Ure2 and CLN-Ure2 before and after digestion with proteinase K

Fibrils were grown by incubation at 37 °C with shaking in 50 mM Tris/HCl buffer (pH 8.4), containing 0.2 M NaCl. Plateau-phase fibrils were digested with 0.1 mg/ml proteinase K for 16 h at 37 °C, harvested by centrifugation, washed and then stained with uranyl acetate. (**a**) Before digestion. The scale bar represents 200 nm. (**b**) After digestion. The scale bar represents 100 nm.

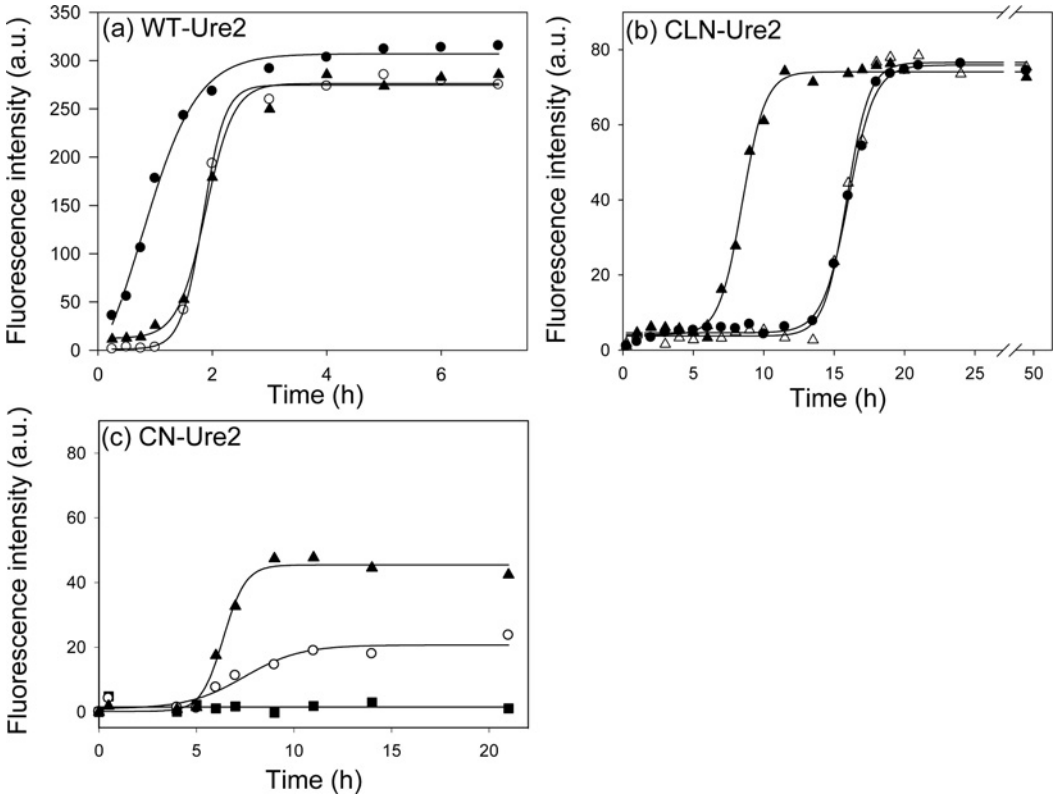

Figure 8 Time course of formation of amyloid-like fibrils by WT-Ure2, CN-Ure2 and CLN-Ure2 monitored by ThT binding

Incubation conditions were 37 °C with shaking in 50 mM Tris/HCl buffer (pH 8.4), containing 0.2 M NaCl. Data points represent the mean of at least three samples incubated in parallel. (**a**) WT-Ure2 (30 μM) was incubated with (●, ▲) or without (○) 5 % preformed fibrillar seeds of WT-Ure2 (●) or CLN-Ure2 (▲). (**b**) CLN-Ure2 (50 μM) was incubated with (●, ▲) or without (△) 5 % preformed fibrillar seeds of WT-Ure2 (●) or CLN-Ure2 (▲). (**c**) CN-Ure2 (50 μM) was incubated in the absence (○) or presence of 0.03 M (▲) or 0.5 M GdmCl (■).

unfolding below 2.0 M GdmCl [21]. However, the GPx activity of Ure2 shows greater sensitivity to GdmCl, with a significant loss of activity above 0.5 M GdmCl (results not shown), which may reflect minor structural changes at the active site and/or inhibition of activity by GdmCl. The reduced ability of CN-Ure2 to form fibrils (Figure 8c), particularly compared with CLN-Ure2 (Figure 8b) which contains a flexible linker (SGSGGGG) between the N- and C-terminal regions (Figure 1), suggests a lack of flexibility in the PrD, or steric hindrance of key amyloid-forming residues due to their proximity of attachment to the globular C-terminal domain, may hinder fibril formation. To test this further, we measured the ability of CN-Ure2 to form fibrils in the presence of low concentrations of GdmCl (0.01−0.5 M). We found that in the presence of very low concentrations of GdmCl (e.g. 0.03 M) the sigmoidal curve for formation of CN-Ure2 monitored by ThT fluorescence showed a significantly higher plateau value (Figure 8c). However, in the presence of higher concentrations of GdmCl (e.g. 0.5 M) fibril formation was inhibited (Figure 8c).

DISCUSSION

A wide range of neurodegenerative diseases including Huntington's disease, Alzheimer's disease, Parkinson's disease and the prion diseases are associated with the misfolding, aggregation and accumulation of specific proteins in neuronal tissue [33]. The protein deposits generally have amyloid-like properties, meaning that they are typically insoluble, protease resistant, contain high β-sheet content, show filamentous morphology and bind Congo Red. The discovery of proteins with prion properties in fungi has contributed significantly to progress in the amyloid field, particularly in the acquirement of structural information about the aggregates and their mechanism of assembly [34]. Yeast provides a powerful genetic model for studying factors that influence prion propagation [35]. In the present study, we used the yeast prion protein Ure2 to study how the relative position of its PrD effects fibril formation *in vitro*.

The *S. cerevisiae* prion state [*URE3*] arises due to aggregation of the Ure2 protein [1]. Similar to many other prion and amyloidogenic proteins, Ure2 assembles readily into protein fibrils *in vitro* [3,4]. Formation of the aggregated prion state of Ure2 *in vivo* depends on the N-terminal PrD [2]. Residues 1−65 of the N-terminal domain are necessary and sufficient to allow generation of Ure2 fibrils, and this region is suggested to constitute the core of the amyloid-like fibrils of Ure2 [3,26]. The remainder of the flexible N-terminal domain (residues 70−90) can be regarded as a linker between the C-terminal domain and the N-terminal domain [26], although in fact this region also contributes to the ability of the protein to induce a prion state when overexpressed in a WT background [17].

In the present study, we found that swapping the relative position of the N- and C-terminal domains of Ure2 to form the variants CLN-Ure2 or CN-Ure2 had no affect on the dimeric structure, overall secondary structural content, thermodynamic stability or enzymatic activity of the native protein (Figures 2−5). CLN-Ure2 and CN-Ure2 showed allosteric enzyme behaviour similar to that of WT-Ure2 in both soluble and fibrillar forms

(Figure 6 and Table 1). This indicates that the GST-like C-terminal domains are retained in a native dimeric configuration within the fibrils of CLN-Ure2 and CN-Ure2, as is the case for WT-Ure2 [14]. The fibrils of CLN-Ure2 and CN-Ure2 showed the same morphology as WT-Ure2 after digestion with proteinase K (Figure 7), suggesting a similar fibril core. The differences between the proteins became apparent, however, when we compared the time course of fibril formation (Figure 8): CLN-Ure2 formed fibrils with a significantly longer lag time than WT-Ure2 and, under the same conditions, CN-Ure2 formed fibrils even less readily, but this could be assisted by addition of extremely low concentrations of the denaturant GdmCl. We also observed that WT- and CLN-Ure2 (or CN-Ure2) were unable to cross-seed, consistent with the differences in fibril architecture that must arise from changing the relative position of the two domains. The results suggest that alteration of the relative positions of the N- and C-terminal domains may affect the availability of key parts of the PrD to make interactions that promote fibril formation. The fact that the addition of low concentrations of chemical denaturant or the insertion of a flexible linker between the two domains facilitated fibril formation suggests that the reduced ability to form fibrils observed for CLN-Ure2 and CN-Ure2 may be primarily due to a lack of flexibility and/or to stearic hindrance.

The results of the present study support previous suggestions that the N- and C-terminal regions of Ure2 are structurally and functionally distinct [2,4,6,15]. The ability of certain proteins to form fibrillar structures is suggested to be an inherent property of the polypeptide backbone [33]. Nevertheless, the ready tendency to form fibrillar structures under mild conditions is confined to a limited subset of proteins. The association between the formation of amyloid-like structures and a range of human diseases, as well as a variety of biological functions in a range of organisms, makes the study of the mechanism and structural properties of amyloid-forming proteins extremely interesting [33,34]. However, obtaining detailed structural information about amyloids has also proven to be extremely challenging [36]. A parallel in-register β-sheet structure has been proposed for Ure2 fibrils, and this structure has been used to explain why the sequence of its N-terminal domain can be shuffled without losing its ability to form fibrils [37]: when the order of the amino acids in the PrD is randomized, the scrambled versions of Ure2 still have the ability to form prions *in vivo* and to form amyloid fibrils *in vitro*, suggesting that prion formation is driven primarily by amino acid composition, largely independent of primary sequence [38].

In the present study, we took the natural protein sequence, but then placed it in an unnatural structural context. The ability of the permutation mutants studied in the present work to form fibrils, but not to cross-seed the WT protein, is also consistent with parallel in-register stacking of β-sheets within the fibril core, and suggests that the direction of alignment of the PrDs is important. Our results are consistent with a model for Ure2 fibril formation in which the PrDs assemble to form an amyloid core, while the native-like globular domains are arranged in an ordered fashion outside this central core. Regarding the contribution of the C-terminal domain to the structure of Ure2 fibrils, and the degree of structural rearrangement that occurs on fibril formation, there has been a certain amount of controversy [23,39−42]. However, there are key aspects on which there is general agreement: (i) the C-terminal domains of Ure2 retain native-like structure and substrate-binding ability within the fibrils [10,13,14,22,25] and (ii) the relative arrangement of individual C-terminal domains within the fibrils of Ure2 is similar to that in the native dimer [14,24]. The observation in the present study of native-like enzymatic activity consistent with allosteric interaction between the dimeric subunits for fibrils of CN-Ure2 and CLN-Ure2 demonstrates that these key features are maintained even when the relative positions of the N- and C-terminal domains of Ure2 are reversed.

AUTHOR CONTRIBUTION

Ming Bai initiated the project and carried out preliminary experiments. Yong Yu and Hai-Yan Wang performed the experiments and helped prepare the manuscript. All authors contributed to experimental design and analysis of the results. Sarah Perrett directed and supervised the research, and wrote the paper.

ACKNOWLEDGEMENTS

We thank Zhongjun Li, Professor Ying Fang and other members of the National Centre for Nanoscience and Technology for advice on fibril sample preparation. We thank Zai-Rong Zhang for assistance with enzyme activity measurements, Yi-Qian Wang for assistance with fibril formation experiments, Dr Xin-Yu Wang and Dr Li-Jun Chen for assistance with use of the Pistar instrument, and the staff of the Institute of Biophysics Electron Microscopy Centre for assistance with electron microscopy experiments.

FUNDING

This work was supported by the National Natural Science Foundation of China [grant numbers 30670428, 30870482 and 31070656]; the Chinese Ministry of Science and Technology [grant numbers 2006CB500703, 2006CB910903]; and the Chinese Academy of Sciences [grant number KSCX2-YW-R-119, KSCX2-YW-R-256].

REFERENCES

1 Wickner, R. B. (1994) [URE3] as an altered URE2 protein: evidence for a prion analog in *Saccharomyces cerevisiae*. Science **264**, 566–569
2 Masison, D. C. and Wickner, R. B. (1995) Prion-inducing domain of yeast Ure2p and protease resistance of Ure2p in prion-containing cells. Science **270**, 93–95
3 Taylor, K. L., Cheng, N., Williams, R. W., Steven, A. C. and Wickner, R. B. (1999) Prion domain initiation of amyloid formation in vitro from native Ure2p. Science **283**, 1339–1343
4 Thual, C., Komar, A. A., Bousset, L., Fernandez-Bellot, E., Cullin, C. and Melki, R. (1999) Structural characterization of Saccharomyces cerevisiae prion-like protein Ure2. J. Biol. Chem. **274**, 13666–13674
5 Thual, C., Bousset, L., Komar, A. A., Walter, S., Buchner, J., Cullin, C. and Melki, R. (2001) Stability, folding, dimerization, and assembly properties of the yeast prion Ure2p. Biochemistry **40**, 1764–1773
6 Perrett, S., Freeman, S. J., Butler, P. J. and Fersht, A. R. (1999) Equilibrium folding properties of the yeast prion protein determinant Ure2. J. Mol. Biol. **290**, 331–345
7 Pierce, M. M., Baxa, U., Steven, A. C., Bax, A. and Wickner, R. B. (2005) Is the prion domain of soluble Ure2p unstructured? Biochemistry **44**, 321–328
8 Bousset, L., Belrhali, H., Janin, J., Melki, R. and Morera, S. (2001) Structure of the globular region of the prion protein Ure2 from the yeast *Saccharomyces cerevisiae*. Structure **9**, 39–46
9 Umland, T. C., Taylor, K. L., Rhee, S., Wickner, R. B. and Davies, D. R. (2001) The crystal structure of the nitrogen regulation fragment of the yeast prion protein Ure2p. Proc. Natl. Acad. Sci. U.S.A. **98**, 1459–1464
10 Zhang, Z. R., Bai, M., Wang, X. Y., Zhou, J. M. and Perrett, S. (2008) 'Restoration' of glutathione transferase activity by single-site mutation of the yeast prion protein Ure2. J. Mol. Biol. **384**, 641–651
11 Courchesne, W. E. and Magasanik, B. (1988) Regulation of nitrogen assimilation in *Saccharomyces cerevisiae*: roles of the URE2 and GLN3 genes. J. Bacteriol. **170**, 708–713
12 Rai, R., Tate, J. J. and Cooper, T. G. (2003) Ure2, a prion precursor with homology to glutathione S-transferase, protects *Saccharomyces cerevisiae* cells from heavy metal ion and oxidant toxicity. J. Biol. Chem. **278**, 12826–12833
13 Bai, M., Zhou, J. M. and Perrett, S. (2004) The yeast prion protein Ure2 shows glutathione peroxidase activity in both native and fibrillar forms. J. Biol. Chem. **279**, 50025–50030
14 Zhang, Z. R. and Perrett, S. (2009) Novel glutaredoxin activity of the yeast prion protein Ure2 reveals a native-like dimer within fibrils. J. Biol. Chem. **284**, 14058–14067
15 Coschigano, P. W. and Magasanik, B. (1991) The URE2 gene product of *Saccharomyces cerevisiae* plays an important role in the cellular response to the nitrogen source and has homology to glutathione S-transferases. Mol. Cell. Biol. **11**, 822–832
16 Shewmaker, F., Mull, L., Nakayashiki, T., Masison, D. C. and Wickner, R. B. (2007) Ure2p function is enhanced by its prion domain in *Saccharomyces cerevisiae*. Genetics **176**, 1557–1565

17 Maddelein, M. L. and Wickner, R. B. (1999) Two prion-inducing regions of Ure2p are nonoverlapping. Mol. Cell. Biol. **19**, 4516–4524
18 Fernandez-Bellot, E., Guillemet, E. and Cullin, C. (2000) The yeast prion [URE3] can be greatly induced by a functional mutated URE2 allele. EMBO J. **19**, 3215–3222
19 Chen, L., Chen, L. J., Wang, H. Y., Wang, Y. Q. and Perrett, S. (2010) Deletion of a Ure2 C-terminal prion-inhibiting region promotes the rate of fibril seed formation and alters interaction with Hsp40. Prot. Eng. Des. Sel. **24**, 69–78
20 Galani, D., Fersht, A. R. and Perrett, S. (2002) Folding of the yeast prion protein Ure2: kinetic evidence for folding and unfolding intermediates. J. Mol. Biol. **315**, 213–227
21 Zhu, L., Zhang, X. J., Wang, L. Y., Zhou, J. M. and Perrett, S. (2003) Relationship between stability of folding intermediates and amyloid formation for the yeast prion Ure2p: a quantitative analysis of the effects of pH and buffer system. J. Mol. Biol. **328**, 235–254
22 Bousset, L., Thomson, N. H., Radford, S. E. and Melki, R. (2002) The yeast prion Ure2p retains its native alpha-helical conformation upon assembly into protein fibrils in vitro. EMBO J. **21**, 2903–2911
23 Baxa, U., Cheng, N., Winkler, D. C., Chiu, T. K., Davies, D. R., Sharma, D., Inouye, H., Kirschner, D. A., Wickner, R. B. and Steven, A. C. (2005) Filaments of the Ure2p prion protein have a cross-β core structure. J. Struct. Biol. **150**, 170–179
24 Fayard, B., Fay, N., David, G., Doucet, J. and Melki, R. (2006) Packing of the prion Ure2p in protein fibrils probed by fluorescence X-ray near-edge structure spectroscopy at sulfur K-edge. J. Mol. Biol. **356**, 843–849
25 Baxa, U., Speransky, V., Steven, A. C. and Wickner, R. B. (2002) Mechanism of inactivation on prion conversion of the *Saccharomyces cerevisiae* Ure2 protein. Proc. Natl. Acad. Sci. U.S.A. **99**, 5253–5260
26 Baxa, U., Taylor, K. L., Wall, J. S., Simon, M. N., Cheng, N., Wickner, R. B. and Steven, A. C. (2003) Architecture of Ure2p prion filaments: the N-terminal domains form a central core fiber. J. Biol. Chem. **278**, 43717–43727
27 Flohe, L. and Gunzler, W. A. (1984) Assays of glutathione peroxidase. Methods Enzymol. **105**, 114–121
28 Holmgren, A. and Aslund, F. (1995) Glutaredoxin. Methods Enzymol. **252**, 283–292
29 Schlumpberger, M., Wille, H., Baldwin, M. A., Butler, D. A., Herskowitz, I. and Prusiner, S. B. (2000) The prion domain of yeast Ure2p induces autocatalytic formation of amyloid fibers by a recombinant fusion protein. Protein Sci. **9**, 440–451
30 Jiang, Y., Li, H., Zhu, L., Zhou, J. M. and Perrett, S. (2004) Amyloid nucleation and hierarchical assembly of Ure2p fibrils. Role of asparagine/glutamine repeat and nonrepeat regions of the prion domains. J. Biol. Chem. **279**, 3361–3369
31 Fei, L. and Perrett, S. (2009) Disulfide bond formation significantly accelerates the assembly of Ure2p fibrils because of the proximity of a potential amyloid stretch. J. Biol. Chem. **284**, 11134–11141
32 Lian, H. Y., Jiang, Y., Zhang, H., Jones, G. W. and Perrett, S. (2006) The yeast prion protein Ure2: structure, function and folding. Biochim. Biophys. Acta **1764**, 535–545
33 Chiti, F. and Dobson, C. M. (2006) Protein misfolding, functional amyloid, and human disease. Annu. Rev. Biochem. **75**, 333–366
34 Perrett, S. and Jones, G. W. (2008) Insights into the mechanism of prion propagation. Curr. Opin. Struct. Biol. **18**, 52–59
35 Jones, G. W. and Tuite, M. F. (2005) Chaperoning prions: the cellular machinery for propagating an infectious protein? BioEssays **27**, 823–832
36 Rambaran, R. N. and Serpell, L. C. (2008) Amyloid fibrils: abnormal protein assembly. Prion **2**, 112–117
37 Ross, E. D., Minton, A. and Wickner, R. B. (2005) Prion domains: sequences, structures and interactions. Nat. Cell Biol. **7**, 1039–1044
38 Ross, E. D., Baxa, U. and Wickner, R. B. (2004) Scrambled prion domains form prions and amyloid. Mol. Cell. Biol. **24**, 7206–7213
39 Speransky, V. V., Taylor, K. L., Edskes, H. K., Wickner, R. B. and Steven, A. C. (2001) Prion filament networks in [URE3] cells of *Saccharomyces cerevisiae*. J. Cell Biol. **153**, 1327–1336
40 Bousset, L., Briki, F., Doucet, J. and Melki, R. (2003) The native-like conformation of Ure2p in fibrils assembled under physiologically relevant conditions switches to an amyloid-like conformation upon heat-treatment of the fibrils. J. Struct. Biol. **141**, 132–142
41 Fay, N., Redeker, V., Savistchenko, J., Dubois, S., Bousset, L. and Melki, R. (2005) Structure of the prion Ure2p in protein fibrils assembled *in vitro*. J. Biol. Chem. **280**, 37149–37158
42 Baxa, U., Wickner, R. B., Steven, A. C., Anderson, D. E., Marekov, L. N., Yau, W. M. and Tycko, R. (2007) Characterization of beta-sheet structure in Ure2p1-89 yeast prion fibrils by solid-state nuclear magnetic resonance. Biochemistry **46**, 13149–13162

Received 16 November 2010; accepted 23 November 2010
Published as BJ Immediate Publication 23 November 2010, doi:10.1042/BJ20101895